

## Article

# Bloom of *Prorocentrum cordatum* in Paracas Bay, Peru

Cecil Tenorio<sup>1,2,3,\*</sup>, Gonzalo Álvarez<sup>2,4,\*</sup>, Melissa Perez-Alania<sup>5</sup>, Jose Luis Blanco<sup>6</sup>, Carlos Paulino<sup>7</sup>, Juan Blanco<sup>8</sup> and Eduardo Uribe<sup>2,3</sup>

- <sup>1</sup> Banco de Germoplasma de Organismos Acuáticos, Instituto del Mar del Perú (IMARPE), Esquina Gamarra y Gral. Valle s/n, Callao 07021, Peru
- <sup>2</sup> Departamento de Acuicultura, Facultad de Ciencias del Mar, Universidad Católica del Norte, Larrondo 1281, Coquimbo 1780000, Chile
- <sup>3</sup> Programa Cooperativo Doctorado en Acuicultura, Universidad Católica del Norte, Larrondo 1281, Coquimbo 1780000, Chile
- <sup>4</sup> Centro de Investigación y Desarrollo Tecnológico en Algas (CIDTA), Facultad de Ciencias del Mar, Universidad Católica del Norte, Larrondo 1281, Coquimbo 1780000, Chile
- <sup>5</sup> Facultad de Ciencias, Universidad Nacional Agraria La Molina, Avenida La Universidad s/n, La Molina, Lima 15024, Peru
- <sup>6</sup> Bluewater Consulting Company, Castro 5700000, Chile
- <sup>7</sup> Dirección General de Investigaciones en Hidroacústica, Sensoramiento Remoto y Artes de Pesca, Instituto del Mar del Perú (IMARPE), Esquina Gamarra y Gral. Valle s/n, Callao 07021, Peru
- <sup>8</sup> Centro de Investigaciones Mariñas (Xunta de Galicia), Pedras de Corón s/n, 36620 Vilanova de Arousa, Pontevedra, Spain
- \* Correspondence: ltenorio@imarpe.gob.pe (C.T.); gmalvarez@ucn.cl (G.Á.);  
Tel.: +51-1-208-8650 (ext. 853) (C.T.); +56-51-220-9766 (G.Á.)

**Abstract:** During the austral winter of 2017, a bloom of *Prorocentrum* spp. occurred, reaching a cell density of  $2.73 \times 10^6$  cells L<sup>-1</sup>, in Paracas Bay, Peru. In order to identify which, type of species generated this event and determine its toxicity, the values of the environmental parameters (temperature, winds and salinity) that induced the rapid growth of the dinoflagellate in this bloom were identified. A clonal culture was established for taxonomic (SEM), phylogenetic (ITS) and toxicological analysis via LC-MS/MS to determine the presence of tetrodotoxin (TTX) and whether the species represents a food safety hazard. This event coincided with the coastal upwelling process, which generated high concentrations of phytoplankton biomass (>10 mg m<sup>-3</sup> chlorophyll-*a*) and allowed the rapid growth of *P. cordatum* (IMP-BG 450) in Paracas Bay. However, toxicological analyses of the IMP-BG 450 strain culture did not show the presence of TTX quantifiable through the technique used. Due to the antecedents of the presence of TTX in mollusks from other latitudes during blooms of this species, it is recommended that analyses of this toxin be carried out both in filter-feeding mollusks and in this species during a new bloom.

**Keywords:** eutrophication; aquaculture; mixotrophic; upwelling



**Citation:** Tenorio, C.; Álvarez, G.; Perez-Alania, M.; Blanco, J.L.; Paulino, C.; Blanco, J.; Uribe, E. Bloom of *Prorocentrum cordatum* in Paracas Bay, Peru. *Diversity* **2022**, *14*, 844. <https://doi.org/10.3390/d14100844>

Academic Editors: Roberto Sandulli and Michael Wink

Received: 31 August 2022

Accepted: 30 September 2022

Published: 6 October 2022

**Publisher's Note:** MDPI stays neutral with regard to jurisdictional claims in published maps and institutional affiliations.



**Copyright:** © 2022 by the authors. Licensee MDPI, Basel, Switzerland. This article is an open access article distributed under the terms and conditions of the Creative Commons Attribution (CC BY) license (<https://creativecommons.org/licenses/by/4.0/>).

## 1. Introduction

The increase in nutrients during recent years in oceanic, continental and estuarial waters due to human activity has favored more intense and frequent harmful algal blooms (HABs) [1]. Together with the effects of climate change and maritime transport, many species have increased their geographic dispersion, leading to a variety of harmful impacts on natural aquatic ecosystems' populations [1–9]. The rise of nutrients in the coastal waters of Peru due to intense upwelling processes [10,11] has increased diatom growth. These blooms have been strongly correlated with the incorporation of NO<sub>3</sub> [4,12–15]. Highly productive aquatic environments are beneficial for invasive species such as those of the genus *Prorocentrum*, with notable increases in their frequency, duration and magnitude in tropical, subtropical and temperate climates alike [16–18].

*Prorocentrum cordatum* (Ostenfeld) J. D. Dodge, 1975 (syn. *Prorocentrum minimum* (Pavillard) Schiller) [19–21]—taxonomically accepted name according to the World Register of Marine Species (WoRMS) [20,22]—presents a global distribution associated with eutrophication, and particularly with nitrogen enrichment [16,18,23], being found near wastewater areas and fish and shrimp farming tanks: all rich in nutrients [4,23,24]. This dinoflagellate has adaptive ecological strategies, such as high intrapopulation variability in the face of environmental stress (eutrophication or pollution) [25,26] and changing its feeding from autotrophy to mixotrophy (phagotrophy) under conditions of low availability of inorganic nutrients, as in the case of the 15 blooms over three decades in the coastal waters of the Baltic Sea where most were of mixotrophic *P. cordatum* [27]. These strategies for its development and maintenance allow this species to be a potential invader and conquer a variety of ecological niches, including coastal ecosystems saturated with species with high anthropogenic nutrient loads [22,28].

*P. cordatum* blooms pose a risk to aquaculture, human health and ecosystems due to their possible link with the presence of tetrodotoxin (TTX) in shellfish [29–32]. The neurotoxin TTX is highly potent, as it can block sodium channels and thereby inhibit the propagation of action potential in muscle and nerve cells [33,34]. In Greece in 2012, TTX was identified in mussels with the presence of *P. minimum* (syn. = *P. cordatum*) [29], and Rodriguez, et al. [35] found TTX analogs in certain strains of *P. minimum* in symbiosis with bacteria (*Roseobacter* and *Vibrio* sp).

*P. cordatum* has been reported on the Peruvian coast but always at a low density ( $<500 \times 10^3$  cells L<sup>-1</sup>) [36–40]. However, between 29 August and 1 September 2017, the HAB monitoring program carried out by the National Fisheries Health Organization (SANIPES) detected a *P. cordatum* bloom in Paracas Bay with a density of  $2.73 \times 10^6$  cells L<sup>-1</sup> (<https://www.sanipes.gob.pe/web/index.php/es/fitoplancton>, accessed on 1 July 2022).

Paracas Bay is a highly productive area in which intense cultivation activity of *Argopecten purpuratus*, and therefore a bloom of a potentially toxic species such as *P. cordatum* can have important consequences for human health and economic activity. The aim of this study was to unequivocally identify the species by morphological and molecular characterization, and to identify the possible presence of TTX, as well as to know if the species represent a food safety hazard.

## 2. Materials and Methods

### 2.1. Environmental Parameters

The data analyzed in this case were temperature (°C), salinity, dissolved oxygen (mg L<sup>-1</sup>), oxygen saturation (%) and phytoplankton density by species (cells L<sup>-1</sup>) from the database of the HAB Monitoring Program in Paracas Bay run by SANIPES from August to September 2017 ([http://desarrollo.sanipes.gob.pe/monitor/grid\\_monitoreo\\_todas/](http://desarrollo.sanipes.gob.pe/monitor/grid_monitoreo_todas/), accessed on 1 July 2022).

#### 2.1.1. Satellite Imagery of Chlorophyll-*a*

Satellite images of surface chlorophyll-*a* concentration were used with 4 km of spatial resolution and level L3 from the timespan of 27 to 29 August 2017, coming from the VIIRS sensor (Visible Infrared Imaging Radiometer Suite) on board the Suomi-NPP satellite (Suomi National Polar-Orbiting Partnership). This information was obtained from the OceanColor web portal (<https://oceancolor.gsfc.nasa.gov/>, accessed on 28 September 2021) operated by NASA (National Aeronautics and Space Administration).

#### 2.1.2. Satellite Wind Imagery

Satellite information about surface wind and speed was used with 25 km of spatial resolution from the following dates: 25 August, 30 August and 1 September 2017. These data comes from the analyses of different satellite wind information sources, published on <https://www.ncei.noaa.gov/products/blended-sea-winds>, (accessed on 28 September

2021) by the National Centers for Environmental Information at NOAA (National Oceanic and Atmospheric Administration).

### 2.1.3. Satellite Sea Surface Temperature

For the SST analysis, daily images of High-Resolution Sea Surface Temperature (GHRSSST) Level 4 were used. These data are produced daily on an operational basis by the JPL OurOcean group using a multi-scale two-dimensional variational (MS-2DVAR) blending algorithm on a global 1 km grid. We selected images of the days 25 and 30 August and 1 September 2017 because they were free of clouds.

### 2.2. Strain Obtention and Culture Conditions

Phytoplankton samples were gathered in August 2017 from Ica in Paracas Bay ( $13^{\circ}49' S$ ,  $76^{\circ}17' W$ ) (Figure 1) via vertical dragging with a conical net ( $10 \mu m$ ). The obtained samples were subsequently transported to the IMARPE laboratory in 250 mL polycarbonate bottles, chilled in ice ( $10^{\circ} C$ ) and protected from sunlight. in order to obtain a monoclonal culture.

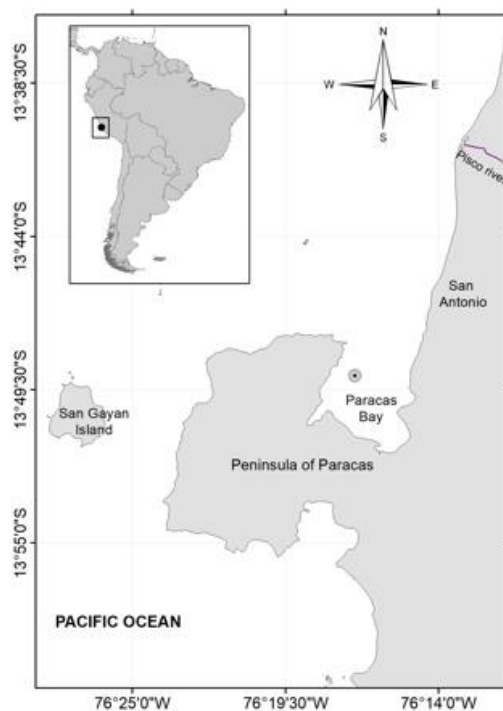


**Figure 1.** Map Paracas Bay, Peru ( $13^{\circ}49' S$ ,  $76^{\circ}17' W$ ).

*P. cordatum* cells were isolated under an inverted phase contrast microscope (NIKON, eclipse TS100, Tokyo, Japan), with the technique of cell washing with micropipettes [41]. The isolated cells were transferred to multiwell culture plates with 2 mL of L1-Si culture medium at a salinity of 32, which were incubated at  $15^{\circ} C$  under a photosynthetically active radiation (PAR) of  $40 \mu mol photons m^{-2} s^{-1}$  and a 12:12 h (light:darkness) photoperiod. The cultures established were transferred to borosilicate Erlenmeyer flasks with 50 mL of L1-Si medium and grown at  $15^{\circ} C$  with a photonic flow of  $80 \mu mol photons m^{-2} s^{-1}$  and a 12:12 h photoperiod (light:darkness). Additional cultures were grown in 1 L borosilicate flasks with an L1-Si medium in the aforementioned conditions with the aim of characterizing the strain.

### 2.3. Morphological Description

Morphometric analysis of cells ( $n = 50$ ) was carried out using an inverted light microscope Zeiss Axio S. A1 with phase contrast, micrography was performed using a Zeiss Axio cam, and cells were analyzed by means of Zen lite software (Zeiss, Oberkochen, Germany).

For scanning electron microscopy (SEM), cells from culture samples in the exponential phase were taken, preserved in 3% glutaraldehyde, washed in distilled water and dehydrated in an ascending ethyl alcohol concentration series (20, 40, 60, 80, 95 and 100%), followed by critical point drying (Tousimis Samdri-780A, Rockville, MA, USA). Dried cells were mounted on a stub and coated with a layer of gold–palladium (JEOL, Tokyo, Japan). Finally, the samples were observed with a scanning electron microscope (Hitachi SU3500, Tokyo, Japan).

#### 2.4. Molecular and Phylogenetic Analysis

##### 2.4.1. DNA and PCR Extraction

To extract genomic DNA, samples were taken from cultures in the exponential growth phase. Cells were concentrated through centrifugation until a pellet was obtained and stored at  $-80\text{ }^{\circ}\text{C}$  for at least 1 hour before DNA extraction. The DNA was extracted via the cetyltrimethylammonium bromide method (CTAB) [42]. Genomic DNA quality and quantification were evaluated using a NanoDrop 2000 spectrophotometer (Thermo Fisher Scientific, Waltham, MA, USA).

The ITS region (ITS1-5.8S-ITS2) was amplified via PCR using ITS1/ITS4 primers [43]. The amplification profile was as follows: initial denaturing at  $95\text{ }^{\circ}\text{C}$  for 3 min, followed by 39 cycles of  $95\text{ }^{\circ}\text{C}$  for 30 s (denaturing),  $56\text{ }^{\circ}\text{C}$  for 30 s (annealing),  $72\text{ }^{\circ}\text{C}$  for 50 s (extension) and a final extension at  $72\text{ }^{\circ}\text{C}$  for 7 min. Amplified products were visualized in agarose gel (1.2%), and were sent to Macrogen Inc. (Seoul, South Korea) to be purified and sequenced for one strand.

##### 2.4.2. Bioinformational Analysis or Phylogenetic Analysis

The sequence obtained was manually edited in BIOEDIT [44] and compared with the public GenBank database via BLASTn to prove its identity. For phylogenetic analyses, 38 sequences were extracted from the GenBank database, including 36 sequences from the genus *Prorocentrum* and 2 sequences from the genera *Takayama* and *Karenia* for the external group (Supplementary Material Table S1). The sequences were aligned using the MUSCLE algorithm (Edgar, 2004) in MEGA 7 v.7.0.26 [45], the alignment was visually corrected and the distances were calculated using the uncorrected *p*-distance model. The final alignment was independently analyzed via neighbor-joining (NJ), maximum likelihood (ML) and Bayesian inference (BI).

The NJ analysis was performed in MEGA 7 using the Kimura-2-parameters model (K2P) with 1000 bootstraps. The best evolutionary model for the phylogenetic analysis (ML and BI) was calculated in jModelTest 2 [46] using the Akaike information criterion (AIC) for ML and the Bayesian information criterion (BIC) for BI. The ML analysis was carried out in RAxML software (v.8.2.X) [47] using the raxmlGUI v.1.5 graphic user interface [48] with the GTR + G model and 1000 repetitions. The BI was conducted in MrBayes v.3.2.6 [49] with the HKY + G model and two parallel analyses, each one with four chains (three hot chains and one cold chain) of 10,000,000 Markov chain Monte Carlo simulations sampled every 1000 generations. The executions' convergence was proven using Tracer v.1.6.0 [50]. The consensus tree was built after a 25% burn-in and subsequent probabilities were estimated.

##### 2.5. Toxin Analysis

The *P. cordatum* culture pellet was obtained based on a culture volume of 500 mL by centrifuging at  $3100\times g$  for 5 minutes using an Eppendorf 810R centrifuge (Hamburg, Germany).

Sample analyses were performed with LC-MS/MS using an Exion AD system (SCIEX, Framingham, MA, USA) coupled with a QTRAP 6500+ triple quadrupole mass spectrometer equipped with an IonDrive TurboV electrospray interface (SCIEX, Framingham, MA, USA). Positive ionization (5500 V),  $650\text{ }^{\circ}\text{C}$  of source temperature, 75 units of GS1 and GS1, 30 units of curtain gas and “medium” collision gas were used. Two MS/MS ionic transitions were monitored for each compound (Table 1).

**Table 1.** Transitions used for TTX and their analogs.

Compound	Transition	Collision Energy
5,6,11-TrideoxyTTX	272.1 > 162.1	40
5,6,11-TrideoxyTTX	272.1 > 254.1	31
11-nor-TTX-6-ol	290.1 > 162.1	40
11-nor-TTX-6-ol	290.1 > 272.1	31
4,9-anhydroTTX	302.1 > 162.1	40
4,9-anhydroTTX	302.101 > 256.1	31
5-deoxyTTX, 11-deoxyTTX	304.1 > 176.1	40
5-deoxyTTX, 11-deoxyTTX	304.1 > 286.1	31
TTX, 4-epiTTX	320.1 > 162.1	40
TTX, 4-epiTTX	320.1 > 302.1	35
C9-265 *	265.1 > 179.1	35
C9-265 *	265.1 > 162.1	40
C9-308 *	308.1 > 180.1	40
C9-308 *	308.1 > 162.1	35

\* Possible TTX analogs [35].

Chromatographic separation was conducted following the method of Boundy, et al. [51]: development of a sensitive and selective method for LC-MS/MS for analyzing the high performance of paralyzing shellfish toxins using solid-phase extraction of graphite carbon.

### 3. Results

#### 3.1. Environmental Parameters

The *P. cordatum* bloom in Paracas Bay during winter 2017 had a density of  $1.11 \times 10^3$  cells  $L^{-1}$  on 25 August, rising to  $2.73 \times 10^6$  cells  $L^{-1}$  on 1 September. Similarly, rises were recorded in water surface temperature ( $>19$  °C) and dissolved oxygen saturation (119%). After 5 September, there was a decrease in the cell density of this dinoflagellate ( $<100 \times 10^3$  cells  $L^{-1}$ ), along with water surface temperature (16 °C) and dissolved oxygen saturation (11%) (Figure 2a,b).

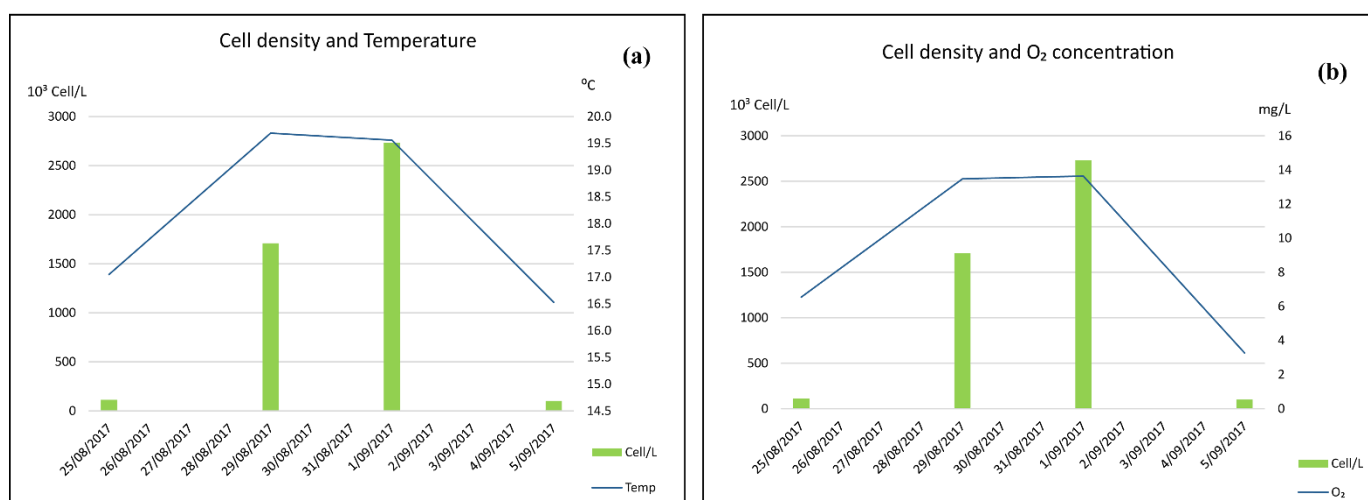


**Figure 2.** (a) Cell density and temperature and (b) cell density and dissolved oxygen from Paracas Bay.

#### 3.1.1. Satellite Chlorophyll-*a*

During the *P. cordatum* bloom, the integrated satellite image of chlorophyll-*a* from 27 to 29 August 2017 shows high concentrations of this photosynthetic pigment ( $>10$  mg  $m^{-3}$ ) in Paracas Bay, extending for around 13 km northwards (Figure 3).

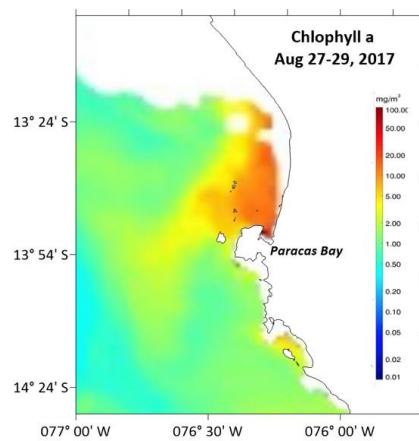


**Figure 3.** Surface distribution of chlorophyll-*a* VIIRS-NPP (27–29 August 2017).

### 3.1.2. Satellite Winds

Coastal winds next to Paracas Bay came from the south and increased their intensity from 25 August ( $6 \text{ m s}^{-1}$ ) to values above  $10 \text{ m s}^{-1}$  by 30 August, before falling to  $5 \text{ m s}^{-1}$  by 1 September (Figure 4a–c).

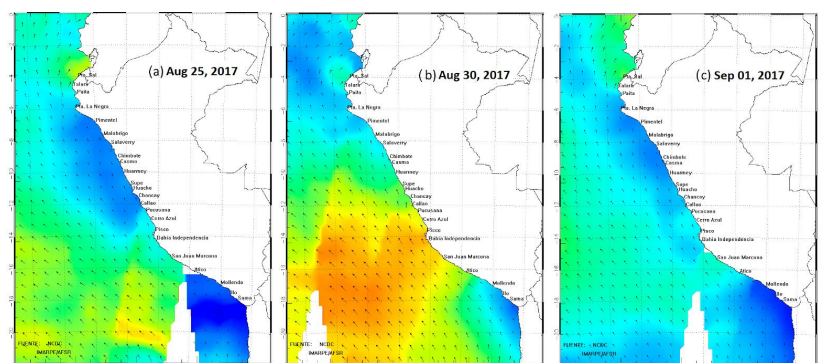


**Figure 4.** Wind speed satellite images ( $\text{m s}^{-1}$ ) (a) 25 August 2017; (b) 30 August 2017; (c) 1 September 2017.

### 3.1.3. Sea Surface Temperature (SST)

Surface temperatures in the southern exterior of Paracas Bay on 25 August were around  $16.5 \text{ }^\circ\text{C}$ , presenting colder waters ( $<16 \text{ }^\circ\text{C}$ ) until 1 September. By contrast, surface temperatures in Paracas Bay and the northern sector were  $17.5 \text{ }^\circ\text{C}$  on 25 August, which rose to  $19.5 \text{ }^\circ\text{C}$  on 29 August and 1 September (Figure 5a–c).

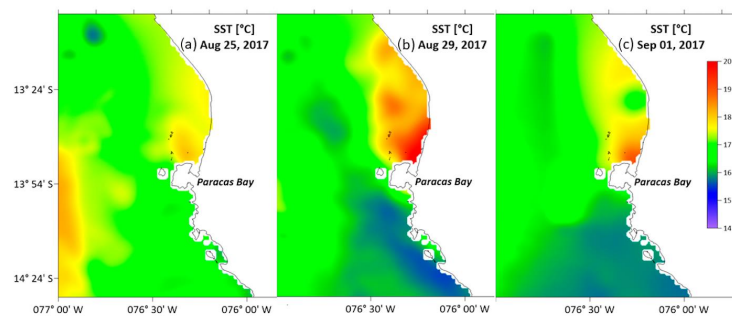


**Figure 5.** Sea surface temperature (SST) in Paracas Bay and environs; (a) 25 August 2017, (b) 30 August 2017 and (c) 1 September 2017 (GHRSSST).

### 3.2. Morphology

The strain isolated from Paracas Bay was coded and morphologically identified as *Prorocentrum cordatum* (Ostenfeld) J. D. Dodge, 1975. The cells of the strain IMP-BG 450 are between 13.8 and 17.2  $\mu\text{m}$  long and 12.7–15.6  $\mu\text{m}$  wide. The cells have round-oval shapes and a high frequency of pentagonal forms (Figure 6a,b), the posterior extreme of the valves is rounded to angled, and the anterior end is straight with a V-shaped central depression and an apical spine. The valves' surfaces are covered with small, pointy spines (250–450 nm) and they also present trichocyst pores (diameter 200 nm). The intercalary band of cells in the growth phase presents spines on both valves; between four and six spines. By contrast, resting phase cells show four spines per valve (Figure 6c). The periflagellar area presents two pores, one smaller circular auxiliary pore (ap) and a longer, larger flagellar pore (fp), all of them surrounded by seven small periflagellar platelets corresponding to 1, 2, 3, 4, 5, 7? and 8 according to classification [52] (Figure 6d). An apical collar measuring 1  $\mu\text{m}$  emerges from the periflagellar plates, along with a robust forked tooth (Figure 6d).

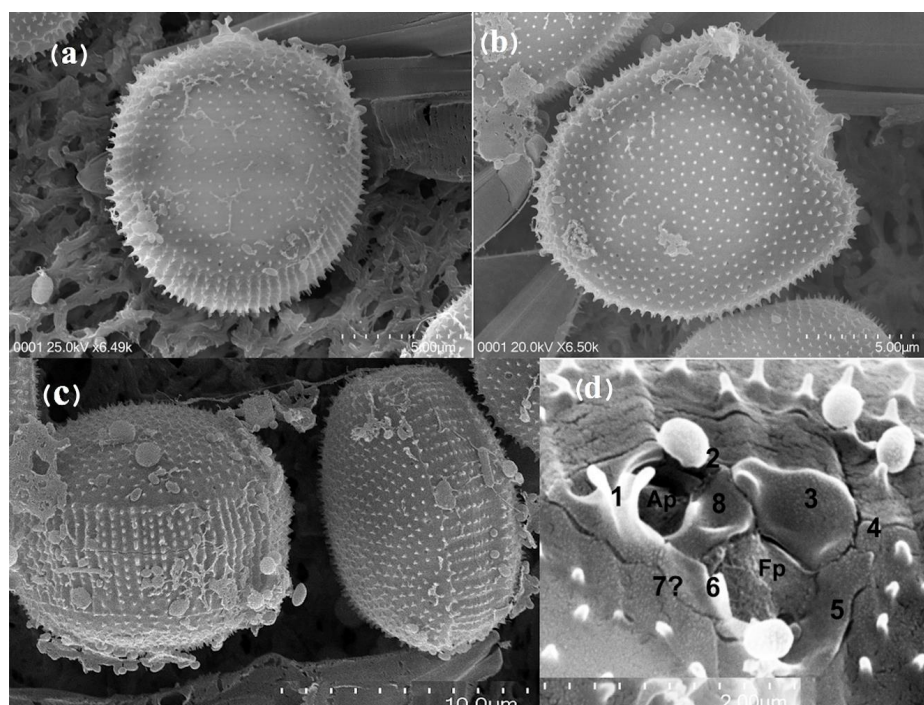


**Figure 6.** Images from scanning electron microscopy (SEM) of the IMP-BG 450 strain of *P. cordatum*; (a) view of the left side valve showing the apical collar, (b) right side valve view, (c) intercalary band and (d) periflagellar platelets (1: forked tooth; 2: small tooth; 3, 4, 5, 6, 7?, 8; Ap: auxiliary pore; Fp: flagellar pore).

### 3.3. Phylogeny

The final alignment had a length of 693 PB and includes 39 sequences from the ITS region (ITS1–5.8S–ITS2) of 507–644 pb. The bloc includes two from the genera *Takayama* and *Karenia* as an external group and 37 sequences from the genus *Prorocentrum*, including the sequence OM812998 (509 pb) from the studied strain IMP BG 450. Except for the difference in the location of one taxon, the phylogenetic trees arising from the Bayesian inference (BI), maximum likelihood (ML) and neighbor-joining (NJ) analyses showed topological congruencies and well-supported grouping (IB = 1.00/ML = 99/NJ = 99) of the study sequence (OM812998), with sequences identified as *P. minimum* (currently *P. cordatum*) showing divergence values (*p*-distance) between 0 and 0.008. The *P. cordatum* cluster includes North Atlantic strains from the USA (CCMP1329, New York; CCMP2233, Delaware; PmiITSC4, North Carolina; CCMP695, CCMP2811, Florida) and Scotland (CCAP1136/16, Argyll); North Pacific strains from Mexico (PIPV-1, Baja California Sur), South Korea (KMMCC

1181, Gyeongnam) and China (PMDH01, Fujian; CCMP2780, Hong Kong Island); and South Pacific strains from Australia (CAWD359, NSW) and Peru (IMP BG 450, Ica) generated in this study (Figure 7).

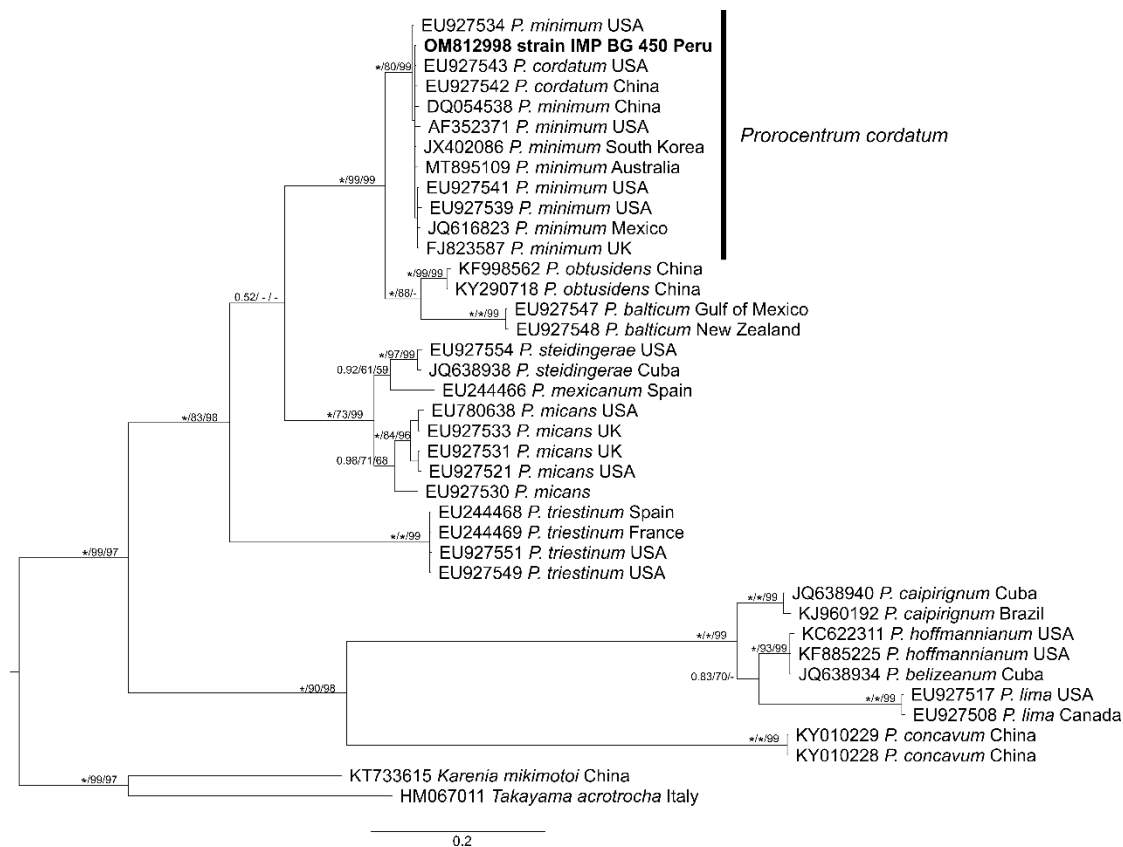


**Figure 7.** *Prorocentrum* Bayesian tree based on ITS sequences. The numbers above lines are nodal supports that indicate Bayesian posterior probabilities (PP), and bootstrap support values from ML and NJ. \* Indicates total support values. “-” Indicates that phylogeny structure for ML or NJ analyses are different at the node. The sequence obtained in this study is indicated in bold.

### 3.4. Toxin Analysis

The *P. cordatum* cultures did not contain tetrodotoxin (TTX) or its analogs in detectable amounts using LC-MS/MS.

## 4. Discussion

### 4.1. Environmental Parameters

The *P. cordatum* bloom ( $2.7 \times 10^6$  cells  $L^{-1}$ ) in Paracas Bay in late winter 2017 was accompanied by species of *Pseudo-nitzschia delicatissima* ( $351 \times 10^3$  cells  $L^{-1}$ ) and *Dinophysis acuminata* ( $11 \times 10^3$  cells  $L^{-1}$ ) (SANIPES). This event is related to increased south winds ( $6 \text{ m s}^{-1}$ ) from 25 to 30 August ( $>10 \text{ m s}^{-1}$ ), corresponding to the strongest coastal winds during the local winter [53,54] and linked to surface water chilling due to upwelling, with an increase in nutrients ( $>10 \mu\text{g L}^{-1}$  of  $\text{N:NO}_3$  and  $>1.5 \mu\text{g L}^{-1}$  of  $\text{P:PO}_4$ ) as well as primary productivity ( $>2000 \text{ mg cm}^2 \text{ day}^{-1}$ ) [55]. *P. cordatum* during the summer of 2014 on the central Peruvian coast presented a high correlation with high nitrate values [36].

This oceanographic process of upwelling, which presents more strongly away from the coast, produces a system of recirculation that provides an optimal environment for a *P. cordatum* bloom in the bay, where high values of surface chlorophyll-*a* ( $>10 \text{ mg m}^{-3}$ ) (Figure 3) with warmer waters ( $>18.5 \text{ }^\circ\text{C}$ ) (Figure 5b,c) extend up to 13 km north of Paracas Bay. A similar distribution structure was presented northwards from Paracas Bay in the late summer of 2015, with a moderate density of *P. cordatum* ( $403 \times 10^3$  cells  $L^{-1}$ ) and low

chlorophyll-*a* values ( $<1 \mu\text{g L}^{-1}$ ) [40]. This low chlorophyll-*a* concentration tends to arise due to the fact that this species is mixotrophic and can feed on particulate matter and prey in a phagotrophic fashion, and thus lacks chlorophyll-*a* [56]. The versatility displayed by *P. cordatum* in obtaining nutrients—whether autotrophic or mixotrophic (phagotrophic), grazing on various species of phytoplankton, as well as being prey for other dinoflagellates and altering the phytoplanktonic community [57]—may be their key to being a successful species in Paracas Bay, increasing the frequency of and prolonging bloom events according to the reports of Glibert and Burkholder [4].

On 4 February 2011 in Paracas Bay, the reported density of *P. cordatum* was  $<200 \times 10^3 \text{ cells L}^{-1}$ . Six years later, in 2017, the first bloom was reported ( $2.720 \times 10^3 \text{ cells L}^{-1}$ ) [58]; a similar timeframe to that reported for the first Baltic Sea bloom by Olenina, et al. [59].

The oceanographical characteristics of Paracas Bay with temperatures ranging from 15–24 °C and salinities between 34 and 35, which are within the eurythermal (3–28 °C) [60–62] and euryhaline (3 and 38) ranges, these are conditions for the abundant growth of *P. cordatum* [28,60,63–67].

Furthermore, human intervention in Paracas Bay and nearby areas (5 to 13 km north) with strong industrial fishing and fish meal processing activity, increases the total available nutrients in this bay [68] and maintaining silt-clay sediments with strong organic loads (5–13%) [69].

There are also large anoxic reaches of the bay, with bottom water OD concentrations between 0.00 and 0.50 mL L<sup>-1</sup> [40].

The nutrient supplies arising from frequent coastal upwelling processes and eutrophication conditions present in Paracas Bay are an optimal environment for the growth of *P. cordatum* and phytoplankton.

These high productivity conditions are favorable for sea bottom aquaculture of *A. purpuratus*, an important economic activity in the area, which could be threatened by the growth of *P. cordatum*. The negative effects of red tides on ocean farming, which generally lead to interruptions due to precautionary closings after these events, would prevent the exploitation of farming resources [61,70–72].

The first reports of *P. cordatum* (as *Exuviaella marina*) in the coastal waters of south-central Peru were reported in 1966 [37], and later became a component of the diet of larval Anchovetas (*Engraulis ringens*) and Sardines (*Sardinops sagax*) [38].

This dinoflagellate was presented in moderate density ( $400 \times 10^3 \text{ cells L}^{-1}$ ) in the Paracas Bay sector during the years 2005–2015 [39,40]. Meanwhile, in Ecuador, this species was detected on four occasions between 2003 and 2004 in the Jambelí Channel and Salado Estuary next to the Gulf of Guayaquil [73].

In the South Atlantic, this species has been reported since 1998 on the Uruguayan coast [74,75]. The highest densities reached in this area have been detected on the northern coastline of the Buenos Aires Province, Argentina, with a maximum concentration of  $\sim 15 \times 10^6 \text{ cells L}^{-1}$ . This event coincided with fish die-offs (Akselman, 1999 in Carreto [76]). During this episode, plankton and bivalve samples demonstrated toxicity in bioassays with mice; however, they were not associated with the presence of *P. minimum* as the cause of the toxicity (Montoya 1998 in [76]).

#### 4.2. Morphology

The present study reports the first detailed taxonomic SEM and phylogenetic study of *P. cordatum* on both the Pacific and Atlantic coasts of South America. The morphological examination of the IMP-BG 450 *P. cordatum* strain presented measurements of 13.8–17.2  $\mu\text{m}$  in length and 12.7–15.6  $\mu\text{m}$  in width when cultivated at 34 PSU, similar to the Chesapeake Bay strain at 14–18  $\mu\text{m}$  length and 13–16  $\mu\text{m}$  width, cultivated at a salinity of 12 PSU. These cell sizes were within the range described by Dodge [77]. Some authors [19,63,64] mention that the variable cell size of this species is related to environmental salinity. However,

Monti-Birkenmeier, et al. [78] state that salinity is not a determining factor for size variation in *P. cordatum*.

Within the taxonomical characteristics of the Paracas Bay *P. cordatum* strain, there were no observations of triangular cells, as described by Martin [79], frequently cited for the Baltic, Caspian Sea, Black Sea and Bulgarian waters [19,77,80,81].

Meanwhile, the round- or oval-shaped *P. cordatum* cells described for this bay are less frequently recorded along the West Coast of the USA, Japan, the Gulf of Mexico, the Gulf of California, the English Channel, the Caspian Sea, the Black Sea and the Mediterranean [19,77,80,82–84].

Furthermore, the pentagonal shape of this IMP-BG450 strain has been described within the morphological variations within the Gulf of Finland [63,80,85].

The intercalary band structure of these *P. cordatum* cells presents four rows of spines, similar to the descriptions by Monti, et al. [86], presenting distancing during the growth phase and without an increase in the number of spine rows. By contrast, the *P. cordatum* in Paracas Bay presented a rise in the number of threads during the growth phase, except for the distancing between them.

The Paracas Bay *P. cordatum* presented eight periflagellar plates, but plate seven was not observed in SEM images. The total number coincides with the observations by Loeblich III [87] and Taylor [88] for this species. A series of spines can be found upon the periflagellum plates, with the most important one being the apical collar described by *P. minimum* (Pavillard) Schiller [19,82,89], and its absence in *P. cordatum* (Ostenfeld) Dodge.

After comparing SEM micrography images of *P. cordatum* from the Baltic Sea [78] and Paracas Bay, we can visualize morphological details of the apical collar presenting a height greater than 1  $\mu\text{m}$ . However, its forms are slightly different for both strains. This taxonomical trait is what separated *P. minimum* from *P. cordatum* [77] as a distinct species. However, greater detail is observed for the apical structure of both strains, with a long thin forked tooth for the Baltic variety, while the one from Paracas Bay is thick and shorter. The valvular spines on the Baltic Sea strains are thick and blunt tipped, while those from Paracas Bay are thin and pointed. The morphological variability present in both strains is related to different environmental conditions as well as genetics.

#### 4.3. Phylogeny

Molecular analyses of the strain (OM812998) IMP-BG450 were carried out based on sequences from the ITS region to confirm the presence of *Prorocentrum cordatum*, (Ostenfeld) J. D. Dodge, 1975, in Paracas Bay. Previously, the ITS region has been useful in recognizing dinoflagellate species [90,91] and *P. cordatum* (as *P. minimum* in McLenna [92]), demonstrating cutoff values at the species level below 0.02 (*p*-distance) for the ITS region in dinoflagellates [91]. The phylogeny obtained shows a well-resolved *P. cordatum* clade with high support and low intra-specific divergence values (<0.02), which groups the studied sequence with exemplars of the species *P. cordatum*, mainly coming from the Northern Hemisphere of the Atlantic and Pacific Oceans, and one recently reported in the South Pacific [92].

#### 4.4. Toxins Analysis

*P. cordatum* strain IMP-BG450 from Paracas Bay did not present TTX, also no intoxications or mortalities were reported in the 2017 bloom, while Vlamis, Katikou, Rodriguez, Rey, Alfonso, Papazachariou, Zacharaki, Botana and Botana [29] detected TTX in mollusks in the presence of *P. cordatum* in Vistonikos Bay, Lagos, Rhodope (Greece).

Toxin production is related to the genetic variability of strains of this species, environmental conditions (temperature, salinity and irradiance) [60] and culture media [16,93], as well as symbiotic association with bacteria (*Roseobacter* and *Vibrio* sp.) [35]. Because of this, the possibility cannot be ruled out that at some moment the conditions may arise to generate toxicity from *P. cordatum* in Paracas Bay.

We suggest that the HAB Monitoring Program should incorporate *P. cordatum* as a hazardous species and carry out toxicological analyses of each event arising on the Peruvian coast, since any harmful species could cause environmental damage and economic loss, implying increased mortality among fish, shellfish and subsequent human poisoning during blooms [16,23,59,61,81,94–96].

## 5. Conclusions

The microalgal bloom of *P. cordatum* in the austral winter of 2017 in Paracas Bay, presented the highest historical density of this species, being stimulated by an intense upwelling process which produced a recirculation towards the interior of Paracas Bay, providing an optimal environment for the bloom.

Taxonomic and molecular analyses indicate the presence of *P. cordatum* in Paracas Bay. It was found that *P. cordatum* during this event did not generate TTX. However, more assays with different factors are needed to evaluate whether the toxins can be expressed in the laboratory. It is suggested to consider the evaluation of TTX analysis in the monitoring carried out by the control entity to avoid problems with this toxin.

**Supplementary Materials:** The following supporting information can be downloaded at: <https://www.mdpi.com/article/10.3390/d14100844/s1>, Table S1: List of *Prorocentrum*, *Takayama* and *Karenia* sequences used in phylogenetic analyses. Strain, collection information and GenBank accession number are presented.

**Author Contributions:** Conceptualization, C.T., G.Á., E.U. and J.B.; methodology, C.T., M.P.-A., G.Á., J.B., C.P., E.U. and J.L.B.; software, C.T., M.P.-A., J.L.B., C.P. and J.B.; investigation, C.T., G.Á., M.P.-A., J.B. and E.U.; formal analysis, C.T., G.Á., M.P.-A., E.U. and J.B.; writing—original draft preparation, C.T., G.Á., M.P.-A., E.U. and J.B.; writing—review and editing, G.Á., E.U. and J.B.; visualization, C.T., G.Á., M.P.-A. and J.B.; supervision, E.U., G.Á. and J.B.; funding acquisition G.Á. and C.T.; All authors have read and agreed to the published version of the manuscript.

**Funding:** This research was funded by the “ANID + FONDEF/PRIMER CONCURSO INVESTIGACIÓN TECNOLÓGICA TEMÁTICO ENSISTEMAS PESQUERO ACUICOLAS FRENTE A FLORECIMIENTOS ALGALES NOCIVOS FANS IDeA DEL FONDO DE FOMENTO AL DESARROLLO CIENTÍFICO Y TECNOLÓGICO, FONDEF/ANID 2017, IT17F10002 developed within the framework of a cooperation agreement between the Consellería do Mar, Xunta de Galicia, Spain and the Universidad Católica del Norte, Chile and the Budget National Program N°094 (PpR094): “Management and Development of Aquaculture”-PRODUCE, PERU, through the project “Technological Development in Aquaculture.

**Institutional Review Board Statement:** Not applicable.

**Data Availability Statement:** Data can be found within the paper and Supplementary Materials.

**Conflicts of Interest:** The authors declare no conflict of interest.

## References

- Glibert, P.M. Harmful algae at the complex nexus of eutrophication and climate change. *Harmful Algae* **2020**, *91*, 101583. [[CrossRef](#)] [[PubMed](#)]
- Anderson, D.M.; Glibert, P.M.; Burkholder, J.M. Harmful algal blooms and eutrophication: Nutrient sources, composition, and consequences. *Estuaries* **2002**, *25*, 704–726. [[CrossRef](#)]
- Hallegraeff, G.M. A review of harmful algal blooms and their apparent global increase. *Phycologia* **1993**, *32*, 79–99. [[CrossRef](#)]
- Glibert, P.M.; Burkholder, J.M. Harmful Algal Species Fact Sheet: *Prorocentrum*. In *Harmful Algal Blooms: A Compendium Desk Reference*; Shumway, S.E., Burkholder, J.M., Morton, S.L., Eds.; Wiley Blackwell: Hoboken, NJ, USA, 2018; pp. 625–628.
- Heisler, J.; Glibert, P.; Burkholder, J.; Anderson, D.; Cochlan, W.; Dennison, W.; Gobler, C.; Dortch, Q.; Heil, C.; Humphries, E.; et al. Eutrophication and Harmful Algal Blooms: A Scientific Consensus. *Harmful Algae* **2008**, *8*, 3–13. [[CrossRef](#)] [[PubMed](#)]
- Anderson, D.M. Toxic algal bloom and red tides: A global perspective. In *Red Tides: Biology, Environmental Science and Technology*; Okaichi, T., Anderson, D.M., Nemoto, T., Eds.; Elsevier: New York, NY, USA, 1989; pp. 11–16.
- Hallegraeff, G.M. Ocean climate change, phytoplankton community responses, and harmful algal blooms: A formidable predictive challenge 1. *J. Phycol.* **2010**, *46*, 220–235. [[CrossRef](#)]

8. Dale, B.; Edwards, M.; Reid, P.C. Climate change and harmful algal blooms. In *Ecology of Harmful Algae*; Springer: Berlin/Heidelberg, Germany, 2006; pp. 367–378.
9. Edwards, M.; Johns, D.G.; Leterme, S.C.; Svendsen, E.; Richardson, A.J. Regional climate change and harmful algal blooms in the northeast Atlantic. *Limnol. Oceanogr.* **2006**, *51*, 820–829. [[CrossRef](#)]
10. Echevin, V.; Gévaudan, M.; Espinoza-Morriberón, D.; Tam, J.; Aumont, O.; Gutierrez, D.; Colas, F. Physical and biogeochemical impacts of RCP8.5 scenario in the Peru upwelling system. *Biogeosciences* **2020**, *17*, 3317–3341. [[CrossRef](#)]
11. Chavez, F.P.; Bertrand, A.; Guevara-Carrasco, R.; Soler, P.; Csirke, J. The northern Humboldt Current System: Brief history, present status and a view towards the future. *Prog. Oceanogr.* **2008**, *79*, 95–105. [[CrossRef](#)]
12. Lomas, M.W.; Glibert, P.M. Interactions between  $\text{NH}_4^+$  and  $\text{NO}_3^-$  uptake and assimilation: Comparison of diatoms and dinoflagellates at several growth temperatures. *Mar. Biol.* **1999**, *3*, 541–551. [[CrossRef](#)]
13. Goldman, J.C. Potential role of large oceanic diatoms in new primary production. *Deep Sea Res. Part I Oceanogr. Res. Pap.* **1993**, *40*, 625–628. [[CrossRef](#)]
14. Kudela, R.M.; Dugdale, R.C. Nutrient regulation of phytoplankton productivity in Monterey Bay, California. *Deep-Sea Res. Part II* **2000**, *47*, 1023–1053. [[CrossRef](#)]
15. Wilkerson, F.P.; Dugdale, R.C.; Kudela, R.M.; Chavez, F.P. Biomass and productivity in Monterey Bay, California: Contribution of the large phytoplankton. *Deep Sea Res. Part II Top. Stud. Oceanogr.* **2000**, *47*, 1003–1022. [[CrossRef](#)]
16. Heil, C.A.; Glibert, P.M.; Fan, C. *Prorocentrum minimum* (Pavillard) Schiller A review of a harmful algal bloom species of growing worldwide importance. *Harmful Algae* **2005**, *4*, 449–470. [[CrossRef](#)]
17. Klanjšček, J.; Geček, S.; Klanjšček, T.; Legović, T. Nutrient quotas and carbon content variability of *Prorocentrum minimum* (Pavillard) Schiller, 1933. *Harmful Algae* **2016**, *51*, 16–25. [[CrossRef](#)] [[PubMed](#)]
18. Glibert, P.M.; Mayorga, E.; Seitzinger, S. *Prorocentrum minimum* tracks anthropogenic nitrogen and phosphorus inputs on a global basis: Application of spatially explicit nutrient export models. *Harmful Algae* **2008**, *8*, 33–38. [[CrossRef](#)]
19. Velikova, V.; Larsen, J. The *Prorocentrum cordatum*/*Prorocentrum minimum* taxonomic problem. *Grana* **1999**, *38*, 108–112. [[CrossRef](#)]
20. Guiry, M.D.; Guiry, G.M. *AlgaeBase*. World-Wide Electronic Publication; National University of Ireland. Galway. Available online: [https://www.algaebase.org/search/species/detail/?species\\_id=71381](https://www.algaebase.org/search/species/detail/?species_id=71381) (accessed on 8 July 2022).
21. Moestrup, O.; Akselmann-Cardella, R.; Churro, C.F.S.; Hoppenrath, M.; Iwataki, M.; Larsen, J.; Lundholm, N.; Zingone, A. IOC-UNESCO Taxonomic Reference List of Harmful Micro Algae. *Prorocentrum cordatum* (Ostenfeld) J.D.Dodge. 1976. Available online: <http://www.marinespecies.org/hab/aphia.php?p=taxdetails&id=232376> (accessed on 8 July 2022).
22. Khanaychenko, A.N.; Telesh, I.V.; Skarlato, S.O. Bloom-forming potentially toxic dinoflagellates *Prorocentrum cordatum* in marine plankton food webs. *Protistology* **2019**, *13*, 95–125. [[CrossRef](#)]
23. Glibert, P.M.; Burkholder, J.M.; Kana, T.M. Recent insights about relationships between nutrient availability, forms, and stoichiometry, and the distribution, ecophysiology, and food web effects of pelagic and benthic *Prorocentrum* species. *Harmful Algae* **2012**, *14*, 231–259. [[CrossRef](#)]
24. Sierra-Beltrán, A.; Cortés-Altamirano, R.; Cortés-Lara, M.d.C. Occurrences of *Prorocentrum minimum* (Pavillard) in México. *Harmful Algae* **2005**, *4*, 507–517. [[CrossRef](#)]
25. Matantseva, O.; Skarlato, S.; Vogts, A.; Pozdnyakov, I.; Liskow, I.; Schubert, H.; Voss, M. Superposition of individual activities: Urea-mediated suppression of nitrate uptake in the dinoflagellate *Prorocentrum minimum* revealed at the population and single-cell levels. *Front. Microbiol.* **2016**, *7*, 1310. [[CrossRef](#)]
26. Telesh, I.V.; Schubert, H.; Skarlato, S.O. Ecological niche partitioning of the invasive dinoflagellate *Prorocentrum minimum* and its native congeners in the Baltic Sea. *Harmful Algae* **2016**, *59*, 100–111. [[CrossRef](#)]
27. Telesh, I.; Schubert, H.; Skarlato, S. Abiotic stability promotes dinoflagellate blooms in marine coastal ecosystems. *Estuar. Coast. Shelf Sci.* **2021**, *251*, 107239. [[CrossRef](#)]
28. Skarlato, S.O.; Telesh, I.V.; Matantseva, O.V.; Pozdnyakov, I.A.; Berdieva, M.A.; Schubert, H.; Filatova, N.A.; Knyazev, N.A.; Pechkovskaya, S.A. Studies of bloom-forming dinoflagellates *Prorocentrum minimum* in fluctuating environment: Contribution to aquatic ecology, cell biology and invasion theory. *Protistology* **2018**, *12*, 113–157. [[CrossRef](#)]
29. Vlamis, A.; Katikou, P.; Rodriguez, I.; Rey, V.; Alfonso, A.; Papazachariou, A.; Zacharaki, T.; Botana, A.M.; Botana, L.M. First detection of tetrodotoxin in Greek shellfish by UPLC-MS/MS potentially linked to the presence of the dinoflagellate *Prorocentrum minimum*. *Toxins* **2015**, *7*, 1779–1807. [[CrossRef](#)]
30. Bordin, P.; Dall’Ara, S.; Tartaglione, L.; Antonelli, P.; Calfapietra, A.; Varriale, F.; Guiatti, D.; Milandri, A.; Dell’Aversano, C.; Arcangeli, G.; et al. First occurrence of tetrodotoxins in bivalve mollusks from Northern Adriatic Sea (Italy). *Food Control* **2021**, *120*, 107510. [[CrossRef](#)]
31. Turner, A.D.; Dhanji-Rapkova, M.; Coates, L.; Bickerstaff, L.; Milligan, S.; O’Neill, A.; Faulkner, D.; McEneny, H.; Baker-Austin, C.; Lees, D.N.; et al. Detection of Tetrodotoxin Shellfish Poisoning (TSP) Toxins and Causative Factors in Bivalve Molluscs from the UK. *Mar. Drugs* **2017**, *15*, 277. [[CrossRef](#)]
32. Gerssen, A.; Bovee, T.; Klijnstra, M.; Poelman, M.; Portier, L.; Hoogenboom, R. First Report on the Occurrence of Tetrodotoxins in Bivalve Mollusks in The Netherlands. *Toxins* **2018**, *10*, 450. [[CrossRef](#)] [[PubMed](#)]
33. Narahashi, T.; Moore, J.W.; Scott, W.R. Tetrodotoxin blockage of sodium conductance increase in lobster giant axons. *J. Gen. Physiol.* **1964**, *47*, 965–974. [[CrossRef](#)] [[PubMed](#)]
34. Narahashi, T. Pharmacology of tetrodotoxin. *J. Toxicol. Toxin Rev.* **2001**, *20*, 67–84. [[CrossRef](#)]

35. Rodríguez, I.; Alfonso, A.; Alonso, E.; Rubiolo, J.A.; Roel, M.; Vlamis, A.; Katikou, P.; Jackson, S.A.; Menon, M.L.; Dobson, A.; et al. The association of bacterial C9-based TTX-like compounds with *Prorocentrum minimum* opens new uncertainties about shellfish seafood safety. *Sci. Rep.* **2017**, *7*, 40880. [CrossRef] [PubMed]
36. Sánchez, S.; Bernales, A.; Delgado, E.; Chang, F.; Jacobo, N.; Quispe, J. Variability and Biogeographical Distribution of Harmful Algal Blooms in Bays of High Productivity off Peruvian Coast (2012–2015). *J. Environ. Anal. Toxicol.* **2017**, *7*, 2161–0525.1000530. [CrossRef]
37. Strickland, J.D.H.; Eppley, R.W.; de Mendiola, B.R. Poblaciones de fitoplancton, nutrientes y fotosíntesis en aguas costeras peruanas. *Bol. Instit. Mar. Perú* **1969**, *2*, 4–45.
38. Muck, P.E.T.E.R.; Rojas de Mendiola, B.; Antonietti, E.M.I.R.A. Comparative studies on feeding in larval anchoveta (*Engraulis ringens*) and sardine (*Sardinops sagax*). In *The Peruvian Upwelling Ecosystem: Dynamics and Interactions*; ICLARM: Manila, Philippines, 1989; Volume 18, pp. 86–96.
39. Solano Cornejo, D.; Mendoza Díaz, V.; CONAM, PNUMA. *Informe Sobre el Estado del Ambiente: GEO Bahía Paracas-Pisco*; Lima, Peru, 2007; pp. 1–163.
40. Sánchez, S.; Jacobo, N.; Bernales, A.; Franco, A.; Quispe, J.; Flores, G. Seasonal variability in the distribution of phytoplankton in Paracas Bay/Peru, as a response to environmental conditions. *J. Environ. Sci. Eng. B* **2018**, 371–380. [CrossRef]
41. Andersen, R.A.; Kawachi, M. Tradiotinal Microalgae Isolation Techniques. In *Algal Culturing Techniques*; Andersen, R.A., Ed.; Elsevier: Amsterdam, The Netherlands, 2005; Volume 578, pp. 83–100.
42. Doyle, J.J.; Doyle, J.L. A rapid DNA isolation procedure for small quantities of fresh leaf tissue. *Phytochem. Bull.* **1987**, *19*, 11–15.
43. White, T.J.; Bruns, T.; Lee, S.; Taylor, J. Amplification and direct sequencing of fungal ribosomal RNA genes for phylogenetics. In *PCR protocols: A Guide to Methods and Applications*; Innis, M., Gelfand, D., Sninsky, J., White, T., Eds.; Academic Press: New York, NY, USA, 1990; pp. 315–322.
44. Hall, T.A. BioEdit: A user-friendly biological sequence alignment editor and analysis program for Windows 95/98/NT. *Nucleic Acids Symp. Ser.* **1999**, *41*, 95–98.
45. Kumar, S.; Stecher, G.; Tamura, K. MEGA7: Molecular evolutionary genetics analysis version 7.0 for bigger datasets. *Mol. Biol. Evol.* **2016**, *33*, 1870–1874. [CrossRef] [PubMed]
46. Darriba, D.; Taboada, G.L.; Doallo, R.; Posada, D. jModelTest 2: More models, new heuristics and parallel computing. *Nat. Methods* **2012**, *9*, 772. [CrossRef] [PubMed]
47. Stamatakis, A. RAxML version 8: A tool for phylogenetic analysis and post-analysis of large phylogenies. *Bioinformatics* **2014**, *30*, 1312–1313. [CrossRef]
48. Silvestro, D.; Michalak, I. raxmlGUI: A graphical front-end for RAxML. *Org. Divers. Evol.* **2012**, *12*, 335–337. [CrossRef]
49. Ronquist, F.; Teslenko, M.; Van Der Mark, P.; Ayres, D.L.; Darling, A.; Höhna, S.; Larget, B.; Liu, L.; Suchard, M.A.; Huelsenbeck, J.P. MrBayes 3.2: Efficient Bayesian phylogenetic inference and model choice across a large model space. *Syst. Biol.* **2012**, *61*, 539–542. [CrossRef]
50. Rambaut, A.; Suchard, M.A.; Xie, D.; Drummond, A.J. Tracer v1. 6. Available online: <http://tree.bio.ed.ac.uk/software/tracer> (accessed on 8 July 2022).
51. Boundy, M.J.; Selwood, A.I.; Harwood, D.T.; McNabb, P.S.; Turner, A.D. Development of a sensitive and selective liquid chromatography-mass spectrometry method for high throughput analysis of paralytic shellfish toxins using graphitised carbon solid phase extraction. *J. Chromatogr. A* **2015**, *1387*, 1–12. [CrossRef] [PubMed]
52. Hoppenrath, M.; Chomérat, N.; Horiguchi, T.; Schweikert, M.; Nagahama, Y.; Murray, S. Taxonomy and phylogeny of the benthic *Prorocentrum* species (Dinophyceae)—A proposal and review. *Harmful Algae* **2013**, *27*, 1–28. [CrossRef]
53. Bakun, A.N.D.R.E.W.; Mendelssohn, R. Alongshore wind stress, 1953–1984: Correction, reconciliation and update through 1986. In *The Peruvian Upwelling Ecosystem: Dynamics and Interactions, Proceedings of the ICLARM Conference Proceedings*; ICLARM: Manila, Philippines, 1989; pp. 77–81.
54. Gutiérrez, D.; Bouloubassi, I.; Sifeddine, A.; Purca, S.; Goubanova, K.; Graco, M.; Field, D.; Méjanelle, L.; Velazco, F.; Lorre, A.; et al. Coastal cooling and increased productivity in the main upwelling zone off Peru since the mid-twentieth century. *Geophys. Res. Lett.* **2011**, *38*, 1–6. [CrossRef]
55. Calienes, R.; Guillén, O.; Lostaunau, N. Variabilidad espacio-temporal de clorofila, producción primaria y nutrientes frente a la costa peruana. *Bol. Inst. Mar. Perú* **1985**, *10*, 1–44.
56. Sukhanova, I.N.; Flint, M.V.; Hibaum, G.; Karamfilov, V.; Kopylov, A.I.; Matveeva, E.; Rat'kova, T.N.; Sazhin, A.F. *Exuviaella cordata* red tide in Bulgarian coastal waters (May to June 1986). *Mar. Biol.* **1988**, *99*, 1–8. [CrossRef]
57. Jeong, H.J.; Du Yoo, Y.; Kim, J.S.; Seong, K.A.; Kang, N.S.; Kim, T.H. Growth, feeding and ecological roles of the mixotrophic and heterotrophic dinoflagellates in marine planktonic food webs. *Ocean. Sci. J.* **2010**, *45*, 65–91. [CrossRef]
58. SANIPES. Fisheries Health Organization of Perú- Organismo Nacional de Sanidad Pesquera. Available online: <https://www.sanipes.gob.pe/web/index.php/es/fitoplancton> (accessed on 8 July 2022).
59. Olenina, I.; Wasmund, N.; Hajdu, S.; Jurgensone, I.; Gromisz, S.; Kownacka, J.; Toming, K.; Vaiciūtė, D.; Olenin, S. Assessing impacts of invasive phytoplankton: The Baltic Sea case. *Mar. Pollut. Bull.* **2010**, *60*, 1691–1700. [CrossRef]
60. Grzebyk, D.; Berland, B. Influences of temperature, salinity and irradiance on growth of *Prorocentrum minimum* (Dinophyceae) from the Mediterranean Sea. *J. Plankton Res.* **1996**, *18*, 1837–1849. [CrossRef]

61. Tango, P.; Magnien, R.; Butler, W.; Luckett, C.; Luckenbach, M.; Lacouture, R.; Poukish, C. Impacts and potential effects due to *Prorocentrum minimum* blooms in Chesapeake Bay. *Harmful Algae* **2005**, *4*, 525–531. [CrossRef]
62. Pertola, S. *Diffusive and Ship-Mediated Spread of Dinoflagellates in the Baltic Sea with Prorocentrum Minimum as a Special Case*; University of Helsinki: Helsinki, Finland, 2006.
63. Hajdu, S.; Edler, L.; Olenina, I.; Witek, B. Spreading and establishment of the potentially toxic dinoflagellate *Prorocentrum minimum* in the Baltic Sea. *Int. Rev. Hydrobiol. A J. Cover. All Asp. Limnol. Mar. Biol.* **2000**, *85*, 561–575.
64. Olenina, I.; Vaičiukynas, E.; Šulčius, S.; Paškauskas, R.; Verikas, A.; Gelžinis, A.; Bačauskienė, M.; Bertašiūtė, V.; Olenin, S. The dinoflagellate *Prorocentrum cordatum* at the edge of the salinity tolerance: The growth is slower but cells are larger. *Estuar. Coast. Shelf Sci.* **2016**, *168*, 71–79. [CrossRef]
65. Knyazev, N.; Pechkovskaya, S.; Skarlato, S.; Telesh, I.; Filatova, N. The impact of temperature stress on DNA and RNA synthesis in potentially toxic dinoflagellates *Prorocentrum minimum*. *J. Evol. Biochem. Physiol.* **2018**, *54*, 383–389. [CrossRef]
66. Pertola, S.; Kuosa, H.; Olsonen, R. Is the invasion of *Prorocentrum minimum* (Dinophyceae) related to the nitrogen enrichment of the Baltic Sea? *Harmful Algae* **2005**, *4*, 481–492. [CrossRef]
67. Kimor, B.; Moigis, A.G.; Dohms, V.; Stienen, C. A case of mass occurrence of *Prorocentrum minimum* in the Kiel Fjord. *Mar. Ecol. Prog. Ser.* **1985**, *27*, 209–215. [CrossRef]
68. Kahru, M.; Michell, B.G.; Diaz, A.; Miura, M. MODIS detects a devastating algal bloom in Paracas Bay, Peru. *Eos Trans. Am. Geophys. Union* **2004**, *85*, 465–472. [CrossRef]
69. IMARPE. Instituto del Mar del Perú. Laboratorio Costero de Pisco. Bases Técnicas Para el Ordenamiento Pesquero y Acuicola de la Bahía Paracas. Available online: <http://www2.produce.gob.pe/RepositorioAPS/3/jer/ACUISUBMENU4/estudios-bahia-paracas.pdf> (accessed on 8 July 2022).
70. Pitcher, G.C.; Bernales Jiménez, A.; Kudela, R.M.; Reguera, B. Harmful algal blooms in Eastern Boundary upwelling systems: A Geohab Core Research Project. *Oceanography* **2017**, *30*, 22. [CrossRef]
71. Dyson, K.; Huppert, D.D. Regional economic impacts of razor clam beach closures due to harmful algal blooms (HABs) on the Pacific coast of Washington. *Harmful Algae* **2010**, *9*, 264–271. [CrossRef]
72. Blanco-Pérez, J. Episodios nocivos por fitoplancton. In *Los Moluscos Pectínidos de Iberoamérica: Ciencia y Acuicultura*; Maeda-Martínez, A.N., Ed.; Limusa: Mexico City, Mexico, 2001; pp. 285–324.
73. Borbor-Cordova, M.J.; Torres, G.; Mantilla-Saltos, G.; Casierra-Tomala, A.; Bermúdez, J.R.; Renteria, W.; Bayot, B. Oceanography of Harmful Algal Blooms on the Ecuadorian Coast (1997–2017): Integrating Remote Sensing and Biological Data. *Front. Mar. Sci.* **2019**, *6*, 13. [CrossRef]
74. Méndez, S.; Ferrari, G. Floraciones algales nocivas en Uruguay: Antecedentes, proyectos en curso y revisión de resultados. In *Floraciones Algas Nocivas en el Cono Sur Americano*; Sar, E.A., Ferrario, M.E., Reguera, B., Eds.; Instituto Español de Oceanografía: Madrid, Spain, 2002; pp. 271–288.
75. Ferrari, G.; Del Carmen Perez, M. Fitoplancton de la costa platense y Atlántica de Uruguay (1993–1994). *Iheringia. Ser. Bot.* **2002**, *57*, 263–278.
76. Carreto, J.I.; Montoya, N.G.; Akselman, R.; Roja, P.M. Proyecto “Protección Ambiental del Río de la Plata y su Frente Marítimo. Prevención y Control de la Contaminación y Restauración de Hábitats” Proyecto PNUD/GEF RLA/99/G31. *RLA* **2004**, *99*, G31.
77. Dodge, J. The Procentrales (Dinophyceae). II. Revision of the taxonomy within the genus *Prorocentrum*. *Bot. J. Linn. Soc.* **1975**, *71*, 103–125. [CrossRef]
78. Monti-Birkenmeier, M.; Berden Zrimec, M.B.; Drinovec, L.; Beran, A.; Zrimec, A.; Cataletto, B.; Fonda Umani, S. Influence of salinity on growth and cell volume in three strains of *Prorocentrum cordatum* (Dinophyceae). *Aquat. Biol.* **2019**, *28*, 1–12. [CrossRef]
79. Martin, G.W. Dinoflagellates from marine and brackish waters of New Jersey. In *University of Iowa Studies in Natural History*; 1929; Volume 12, pp. 3–32.
80. Pertola, S.; Faust, M.A.; Kuosa, H.; Hallfors, G. Morphology of *Prorocentrum minimum* (Dinophyceae) in the Baltic Sea and in Chesapeake Bay: Comparison of Cell Shapes and Thecal Ornamentation. *Bot. Mar.* **2003**, *46*, 477–486. [CrossRef]
81. Witek, B.; Plinski, M. The first recorded bloom of *Prorocentrum minimum* (Pavillard) Schiller in the coastal zone of the Gulf of Gdańsk. *Oceanologia* **2000**, *42*, 29–36.
82. Marasović, I.; Pucher-Petković, T.; Petrova-Karadjova, V. *Prorocentrum minimum* (Dinophyceae) in the Adriatic and Black sea. *J. Mar. Biolog. Assoc. UK* **1990**, *70*, 473–476. [CrossRef]
83. Muciño-Márquez, R.E.; Gárate-Lizárraga, I.; López-Cortés, D.J. Seasonal Variation of the Genus *Prorocentrum* (Dinophyceae) in Two Tuna Farms in the Bahía De La Paz, Mexico. *Acta Biol. Colomb.* **2014**, *20*, 195–206. [CrossRef]
84. Petrova, D.; Gerdzhikov, D. Development of a traditional blooming phytoplankton species *Prorocentrum cordatum* Dodge, 1975 along the Bulgarian coast (2008–2010). In *Proceedings of the Union of Scientists in Bulgaria-Varna, Series “Marine Science”*, Bulgaria, Varna, 2013; pp. 12–17.
85. Hajdu, S.; Pertola, S.; Kuosa, H. *Prorocentrum minimum* (Dinophyceae) in the Baltic Sea: Morphology, occurrence—A review. *Harmful Algae* **2005**, *4*, 471–480. [CrossRef]
86. Monti, M.; Stoecker, D.K.; Cataletto, B.; Talarico, L. Morphology of the flagellar pore complex in *Prorocentrum minimum* (Dinophyceae) from the Adriatic and Baltic Seas. *Bot. Mar.* **2010**, *53*. [CrossRef]
87. Loeblich, A.R., III. Dinoflagellate evolution: Speculation and evidence. *J. Protozool.* **1976**, *23*, 13–28. [CrossRef]
88. Taylor, F. On dinoflagellate evolution. *BioSystems* **1980**, *13*, 65–108. [CrossRef]

89. Taylor, F.; Fukuyo, Y.; Larsen, J.; Hallegraeff, G. Taxonomy of harmful dinoflagellates. In *Harmful Marine Microalgae*; Hallegraeff, G.M., Anderson, D.M., Cembella, A.D., Eds.; UNESCO: Paris, France, 2003; pp. 389–482.
90. Wayne Litaker, R.; Vandersea, M.W.; Kibler, S.R.; Reece, K.S.; Stokes, N.A.; Lutzoni, F.M.; Yonish, B.A.; West, M.A.; Black, M.N.D.; Tester, P.A. Recognizing Dinoflagellate species using ITS rDNA sequences. *J. Phycol.* **2007**, *43*, 344–355. [[CrossRef](#)]
91. Stern, R.F.; Andersen, R.A.; Jameson, I.; Küpper, F.C.; Coffroth, M.A.; Vaultot, D.; Le Gall, F.; Véron, B.; Brand, J.J.; Skelton, H.; et al. Evaluating the ribosomal internal transcribed spacer (ITS) as a candidate dinoflagellate barcode marker. *PLoS ONE* **2012**, *7*, e42780. [[CrossRef](#)] [[PubMed](#)]
92. McLennan, K.; Ruvindy, R.; Ostrowski, M.; Murray, S. Assessing the Use of Molecular Barcoding and qPCR for Investigating the Ecology of *Prorocentrum minimum* (Dinophyceae), a Harmful Algal Species. *Microorganisms* **2021**, *9*, 510. [[CrossRef](#)] [[PubMed](#)]
93. Nakazima, M. Studies on the source of shellfish poison in Lake Hamana. III. Poisonous effects of shellfish feeding on *Prorocentrum* sp. *Bull. Jpn. Soc. Sci. Fish* **1965**, *31*, 281–285. [[CrossRef](#)]
94. Al-Hashmi, K.A.; Smith, S.L.; Claereboudt, M.; Piontkovski, S.A.; Al-Azri, A. Dynamics of potentially harmful phytoplankton in a semi-enclosed bay in the Sea of Oman. *Bull. Mar. Sci.* **2015**, *91*, 141–166. [[CrossRef](#)]
95. Denardou Queneherve, A.; Grzebyk, D.; Pouchus, Y.F.; Sauviat, M.P.; Alliot, E.; Biard, J.F.; Berland, B.; Verbist, J.F. Toxicity of French strains of the dinoflagellate *Prorocentrum minimum* experimental and natural contaminations of mussels. *Toxicon* **1999**, *37*, 1711–1719. [[CrossRef](#)]
96. Wikfors, G.H.; Smolowitz, R.M. Experimental and histological studies of four life-history stages of the eastern oyster, *Crassostrea virginica*, exposed to a cultured strain of the dinoflagellate *Prorocentrum minimum*. *Biol. Bull.* **1995**, *188*, 313–328. [[CrossRef](#)]